Increasing Protein Charge State When Using Laser Electrospray Mass Spectrometry

ARTICLE *in* JOURNAL OF THE AMERICAN SOCIETY FOR MASS SPECTROMETRY · MARCH 2015

Impact Factor: 2.95 · DOI: 10.1007/s13361-015-1084-3 · Source: PubMed

5 AUTHORS, INCLUDING:

Santosh Karki

Temple University

5 PUBLICATIONS **23** CITATIONS

SEE PROFILE

Paul M. Flanigan

Signature Science, LLC

16 PUBLICATIONS **102** CITATIONS

SEE PROFILE

J. Am. Soc. Mass Spectrom. (2015) 26:706–715
DOI: 10.1007/s13361-015-1084-3

RESEARCH ARTICLE

Increasing Protein Charge State When Using Laser Electrospray Mass Spectrometry

Santosh Karki, Paul M. Flanigan IV, Johnny J. Perez, Jieutonne J. Archer, Robert J. Levis

Department of Chemistry and Center for Advanced Photonics Research, Temple University, Philadelphia, PA 19122, USA

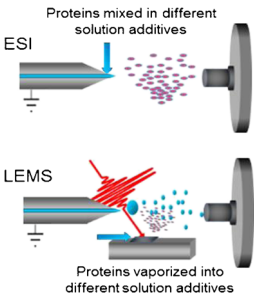

Abstract. Femtosecond (fs) laser vaporization is used to transfer cytochrome *c*, myoglobin, lysozyme, and ubiquitin from the condensed phase into an electrospray (ES) plume consisting of a mixture of a supercharging reagent, *m*-nitrobenzyl alcohol (*m*-NBA), and trifluoroacetic acid (TFA), acetic acid (AA), or formic acid (FA). Interaction of acid-sensitive proteins like cytochrome *c* and myoglobin with the highly charged ES droplets resulted in a shift to higher charge states in comparison with acid-stable proteins like lysozyme and ubiquitin. Laser electrospray mass spectrometry (LEMS) measurements showed an increase in both the average charge states (Z_{avg}) and the charge state with maximum intensity (Z_{mode}) for acid-sensitive proteins compared with conventional electrospray ionization mass spectrometry (ESI-MS) under equivalent solvent conditions. A marked increase in ion abundance of higher charge states was observed for LEMS in comparison with conventional electrospray for cytochrome *c* (ranging from 19+ to 21+ versus 13+ to 16+) and myoglobin (ranging from 19+ to 26+ versus 18+ to 21+) using an ES solution containing *m*-NBA and TFA. LEMS measurements as a function of electrospray flow rate yielded increasing charge states with decreasing flow rates for cytochrome *c* and myoglobin.

Keywords: Femtosecond, Laser, Electrospray ionization, Supercharging, Charge state distribution

Received: 23 June 2014/Revised: 20 January 2015/Accepted: 22 January 2015/Published Online: 10 March 2015

Introduction

Electrospray ionization of proteins generates multiply charged gas phase ions with a charge state distribution (CSD) characteristic of the extent of denaturation [1]. One of the factors that affects the CSD is the configuration of the protein in the solution phase prior to transfer to the gas phase [1, 2]. A protein in its native configuration displays a narrow range of lower charge states because the amino acid side chains in the folded protein are protected from the solvent environment and lack the ability to pick up additional charge. A higher range of charge states typically results from an extended (unfolded) protein conformation where the amino acid side chains are exposed to the solvent and, thus, can accommodate more charge. In addition to protein conformation, other factors affect the CSD including gas phase basicity of the analyte and solvent [3–5], presence of supercharging reagents [6–9], instrument settings, and desolvation processes [10].

Increasing the number of charges on a given protein can be achieved either by adding protein to an acidic solution prior to electrospraying [2] or by exposing electrospray (ES) droplets containing protein molecules to acid vapors in the region between the spray tip and the MS inlet [11, 12]. During the desolvation process, the ES droplets are enriched with acid content because of the faster evaporation rate of electrospray solvents such as water and methanol in comparison with an acid (e.g., acetic acid). An increase in the acid concentration lowers the droplet pH and provides a favorable condition for denaturation and increase in protein charging. In addition to increasing ion charge, interaction of protein molecules with acid vapors also helps to improve the ES signal response and to prevent the dissociation of noncovalent complexes resulting from a denaturing ES solvent prior to mass analysis [12]. A reduction in the average charge state, Z_{avg}, can be accomplished using basic vapors, and using extractive electrospray ionization (EESI) [13] and electrosonic spray ionization (ESSI) [14] have also been reported. For example, in EESI, the basic reagent nebulized by the nitrogen gas interacts with the ES stream containing multiply charged protein ions, allowing ion/molecule reactions to reduce Z_{avg}.

Supercharging reagents, such as *m*-nitro benzyl alcohol (*m*-NBA), can also be employed to enhance charging of proteins.

Electronic supplementary material The online version of this article (doi:10.1007/s13361-015-1084-3) contains supplementary material, which is available to authorized users.

Correspondence to: Robert J. Levis; *e-mail:* rjlevis@temple.edu

The low vapor pressure of *m*-NBA compared with conventional electrospray solvents results in an increased concentration of supercharging reagent in the droplet at the end of the desolvation process. This will change the properties of the droplet, which may result in chemical and/or thermal denaturation, although this has been a subject of debate [15–18]. The change in protein conformation during the supercharging event is likely to be protein-dependent [19]. An investigation of the σ^{54} activator protein complex revealed a decrease in relative abundance of high-order complexes (heptamer, tetramer, trimer, and dimer) with a simultaneous increase in monomer abundance with increasing *m*-NBA concentration, suggesting a change in the structure due to partial dissociation of the complex [18]. Conversely, using a supercharging reagent resulted in an increase in the average charge of phosphorylase b dimer (195 kDa) without the disruption of dimer complex suggesting that supercharging occurs without significant structural modification [16]. There are several merits associated with obtaining higher charge states. Enhanced charging of large biomolecules has been shown to be of value for performing high mass accuracy (sub-ppm) measurements [20, 21] and for improving the efficiency of electron-based tandem mass spectrometry (MS/MS) techniques for molecular sequencing experiments [22–25]. Increasing the protein ion charge state is important for performing top-down proteomics because the greater the charge state, the more rapid the dissociation during the MS/MS experiments giving rise to more useful information on the molecular sequence and structure of macromolecules [26].

The interaction of laser-desorbed proteins with the ES droplets containing a supercharging reagent can increase protein charge states, as shown by electrospray-assisted laser desorption/ionization (ELDI) measurements [27]. The ELDI process, employing a UV laser for desorption of dried proteins into ES droplets containing *m*-NBA, was utilized for the online supercharging of human insulin and bovine carbonic anhydrase, resulting in an increase in the average charge state from 4.0 to 4.8 and from 27.7 to 30.0, respectively. Besides ELDI, several other laser-based ionization techniques, such as laser ablation electrospray ionization (LAESI) [28], infrared laser-assisted desorption electrospray ionization (IR LADESI) [29], infrared laser desorption electrospray ionization (IR-LDESI) [30], matrix assisted laser desorption spray post-ionization mass spectrometry (LDSPI-MS) [31], and matrix-assisted laser desorption electrospray ionization (MALDESI) [32] have been developed. All these ambient ionization methods utilize a laser to desorb or ablate either liquid or solid samples followed by electrospray post-ionization. A detailed review of ambient laser mass spectrometry techniques has recently been published [33].

A recently developed atmospheric pressure ionization technique, (LEMS) [34], has enabled rapid analysis of large biomolecules and complex mixtures without pre-processing steps such as deposition of matrix, extraction from a homogenized sample, or placement into vacuum. LEMS couples nonresonant femtosecond (fs) laser vaporization with ES ionization to perform ambient pressure mass analysis on a wide variety of samples, including pharmaceuticals [35], lipids [36], narcotics [37], dipeptides [34], explosives [38–40], and plant tissues [41, 42] for phenotype classification [41]. Most importantly, investigations of lysozyme and cytochrome *c* revealed that the solution-phase conformation was preserved during transfer to ES droplets when an intense, nonresonant ultrafast laser was employed for vaporization [43]. Previous LEMS investigations suggested that the reduced interaction time of the laser vaporized analytes with the ES droplets limits partitioning into the interior of the droplet [43–45]. This would allow vaporized analytes to preferentially interact with the surface of the ES droplet where charges reside. This nonequilibrium partitioning of laser vaporized proteins could facilitate a larger yield of higher charge states when subjected to highly acidic solvent conditions combined with a supercharging reagent, creating optimal conditions for performing electron-based tandem mass spectrometry (MS/MS) for top-down sequencing.

Here, we investigate nonresonant femtosecond laser vaporization of proteins into electrospray solvents containing a supercharging reagent (*m*-NBA) and trifluoroacetic acid (TFA), acetic acid (AA), or formic acid (FA). We report the mass spectral charge state distributions for cytochrome *c*, myoglobin, lysozyme, and ubiquitin as a function of acid concentration in ES solution. The charge state distributions are compared for laser vaporization ES post-ionization and conventional ESI analyses. Charge state distributions were also measured as a function of electrospray solvent flow rate.

Materials and Methods

Sample Preparation

Solid samples of cytochrome *c* and myoglobin from horse heart, ubiquitin from bovine erythrocytes, and liquid samples of *m*-NBA and trifluoroacetic acid were purchased from Sigma Aldrich (St. Louis, MO, USA). Solid hen egg lysozyme was purchased from USB Corporation (Cleveland, OH, USA). Liquid samples of acetic acid and formic acid were purchased from J. T. Baker (Phillipsburg, NJ, USA). All analytes and reagents were used without further purification. For conventional ESI-MS of cytochrome *c*, myoglobin, lysozyme, and ubiquitin, a 1×10^{-3} M stock solution of each protein was prepared in HPLC grade water (Fisher Scientific, Pittsburgh, PA, USA). An aliquot of the stock solution was then diluted into 1:1 (v:v) water:methanol to yield a final protein concentration of 1×10^{-5} M. Three 1:1 (v:v) water:methanol ESI solutions were utilized in this study. These ESI solutions included 0.4% *m*-NBA with 0.1% trifluoroacetic acid, 0.1% acetic acid, or 0.1% formic acid. For LEMS analysis, 10 μL of the stock protein solution spotted on a stainless steel plate was vaporized from solution into the same ES solvents used for conventional ESI-MS but without any protein.

Laser Vaporization and Ionization System

A Ti:sapphire laser oscillator (KM Laboratories, Inc., Boulder, CO, USA) seeded a regenerative amplifier (Coherent, Inc., Santa Clara, CA, USA) for the creation of 75 fs, 2.0 mJ laser pulses centered at 800 nm. The laser, operated at 10 Hz to couple with the ES ion source, was focused to a spot size of ~350 μm in diameter with an incident angle of 45° with respect to the sample using a 16.9 cm focal length lens, with an approximate intensity of 2×10^{13} W/cm^2. The steel sample plate was biased to –2.0 kV to compensate for the distortion of electric field between the capillary and the needle caused by the sample stage. The area sampled was 6.4 mm below and approximately 1 mm in front of the ES needle. Aqueous protein sample (10 μL) deposited on the steel substrate was vaporized by the intense pulses allowing for capture and ionization by an ES plume traveling perpendicular to the vaporized material. The flow rate for ES solvent was typically set at 3 μL/min by a syringe pump (Harvard Apparatus, Holliston, MA, USA), except for the flow rate study. The charged droplets containing captured analytes were dried by counter-propagating nitrogen gas at 180°C during transit to the MS inlet.

Mass Spectrometry and Data Analysis

The mass spectrometer used in this experiment has been previously described [34]. The system combines an intense nonresonant femtosecond laser pulse that enables transference of the analytes into the gas phase for capture and ionization in an ES plume at atmospheric pressure. The ES ionization source (Analytica of Branford, Inc., Branford, CT, USA) operated in a configuration to generate positive ions consists of an ES needle, dielectric capillary, skimmer, and hexapole. The ES needle was maintained at ground while the inlet capillary was biased to –4.5 kV to operate in positive ion mode. The ESI needle was 6.4 mm above, and parallel to, the sample stage and was approximately 6.4 mm in front of the capillary entrance. The hexapole was operated in the trapping mode, where the positive ions were collected at 10 Hz. After exiting the ESI source, the ions were transferred to the extraction region by a second hexapole, where they were injected orthogonally into the linear time-of-flight analyzer and extracted via two high voltage pulsers (Directed Energy Inc., Fort Collins, CO, USA, and Quantum Technology Inc., Lake Mary, FL, USA) that were triggered 210 μs after the ions exit the first hexapole. The positive ions were then detected, and the resulting mass spectra were averaged for 5 s for ESI and (50 laser shots) LEMS analysis.

The raw mass spectral data files were imported into the Cutter program [46] for integration of the protein features. Baseline subtraction and spectral realignment were performed before integration to ensure consistent integration. The average charge state (Z_{avg}) was calculated using Eq. (1), where q_i is the net charge, W_i is the sum of signal intensity of the i^{th} charge state, and N is the number of charge states present in the mass spectra. The charge state with maximum intensity (Z_{mode}) was determined from the average of seven mass spectra.

$$Z_{avg} = \frac{\sum_i^N q_i w_i}{\sum_i^N w_i} \quad (1)$$

Results and Discussion

Analysis of Acid Sensitive Proteins (Cytochrome c and Myoglobin)

Cytochrome c Cytochrome c is a small globular protein that contains a covalently bound heme group. The ESI-MS CSD of cytochrome *c* has been shown to correlate with solution phase conformation [2]. The native configuration of the protein results in a narrow range of charge states (mostly 8+ and 7+) at high *m/z* ratio as shown by nano-ESI-MS experiments [47], whereas the broad range of charge states centered around 12+ is indicative of the unfolded configuration [47, 48]. The conventional ESI mass spectra of cytochrome *c* measured in solvent containing a mixture of *m*-NBA with TFA, AA, or FA are shown in Fig. 1a, b, and c, respectively. The measurements reveal monomodal CSDs with most abundant charge states (Z_{mode}) of 14+, 18+, and 19+ for TFA, AA, and FA, respectively. An increase in protein charge was achieved using a solvent containing either an acid or *m*-NBA in comparison with buffered water:methanol (Figure S1 in Supporting Information), but the solvents combining both an acid and *m*-NBA resulted in larger increase in ion intensities of the higher charge states than either alone. The highest charge state (Z_{max}) observed in the mass spectra was 23+ for all three electrospray solvents, whereas the lowest charge state (Z_{min}) observed was 8+ for TFA and AA with *m*-NBA, and 10+ for FA with *m*-NBA. The broad range and increased abundance of higher charge states indicate that the cytochrome *c* unfolds as the result of the denaturing solvent containing acid and *m*-NBA. The mean of the CSD (Z_{avg}) and the charge states with maximum intensity (Z_{mode}) resulting from the analysis of the four proteins with different electrospray solvents are shown in Table 1.

The variation in protein charge states (Z_{avg} and Z_{mode}) presumably arise from the pK_a, boiling point, and/or the surface tension of the acids (Table 2). A correlation between the CSD shift of cytochrome *c* with the strength of the acid was previously reported by studying the effect of acid vapors leaked into the ESI interface [12]. However, neither Z_{avg} nor Z_{mode} correlated to acid strength in this study. Trifluoroacetic acid is the strongest acid, followed by formic acid and acetic acid (pKa values of 0.52, 3.75, and 4.76, respectively). FA, followed by AA, provided the highest Z_{avg} and a larger increase in ion intensity of higher charge states compared with TFA. The discrepancy in the Z_{avg} as a function of pK_a might be due to the difference in other physiochemical properties of the acids, such as boiling point, ion pairing ability, and the surface

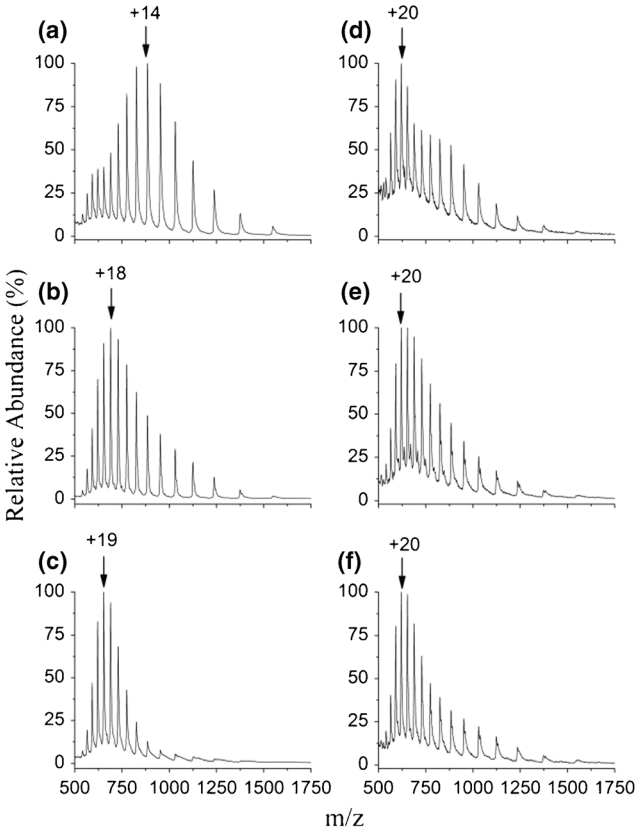

Figure 1. Mass spectra representing ES of cytochrome *c* prepared in 1:1 (v:v) water:methanol with 0.4% *m*-NBA and 0.1% (**a**) trifluoroacetic acid, (**b**) acetic acid, and (**c**) formic acid; (**d**), (**e**), (**f**) represent laser induced vaporization of cytochrome *c* into the ES solvent consisting of 1:1 (v:v) water:methanol with 0.4% *m*-NBA and 0.1% trifluoroacetic acid, acetic acid, and formic acid, respectively. The pH of the solution was measured to be 2.2 with trifluoroacetic acid, 2.9 with acetic acid, and 2.5 with formic acid

tension. Trifluoroacetic acid has a lower boiling point than water and will evaporate during desolvation, resulting in an increase in droplet pH compared with that of the starting solution, lowering the proton concentration at the droplet surface. Acetic acid has a higher boiling point than water, and during solvent evaporation, the ES droplets likely become enriched with acetic acid, increasing the proton concentration. In addition to the proton density, the nature of the anionic species present in the solution may also affect the distribution of protein charge states. Anions can pair with positively charged basic amino acids of the protein in the solution phase and reduce the total number of charges on a protein molecule [49]. The stability of the adduct ($R\text{-}NH_2^{\cdots}H^{+\cdots}A^-$) formed depends on the gas-phase basicity of the amino group and the attaching anion [50]. The limited resolution of the mass spectrometer does not enable the identification of adducts in this experiment. The CF_3COO^- anion (TFA) has a greater propensity to form an ion pair in comparison with CH_3COO^- anion (AA), which results in greater ion suppression effects. The increase in Z_{avg} for cytochrome *c* for *m*-NBA and FA in comparison with *m*-NBA and AA is most likely due to the pKa and/or the surface tension values of these acids.

Laser vaporization of aqueous cytochrome *c* into electrospray solutions consisting of 1:1 (v:v) water:methanol with *m*-NBA and TFA, AA, or FA was performed to investigate the nonequilibrium partitioning effect on Z_{avg} or the relative abundance of the higher charge states. The LEMS measurements for cytochrome *c* with *m*-NBA and TFA (Fig. 1d), AA (Fig. 1e), and FA (Fig. 1f) displayed monomodal CSDs with Z_{mode} values of 20+. The Z_{max} and Z_{min} observed in the mass spectra were 24+ and 8+, respectively, for all three electrospray solvent conditions. Previous investigations of cytochrome *c*, laser vaporized into a buffered water:methanol ESI solution, showed a Z_{mode} of 7+ [43] (Figure S1a in Supporting Information). The high charge states observed from the interaction of laser vaporized folded cytochrome *c* with the denaturing electrospray solvents in this study suggests a conformational change in the protein. The Z_{avg} for the LEMS measurements in comparison with the ESI-MS measurements were: 16.3±0.3 versus 14.5±0.1 for TFA, 16.5±0.5 versus 16.2±0.1 for AA, and 16.8±0.3 versus 17.8±0.1 for FA, as seen in Table 1. The fact that the Z_{avg} values for LEMS measurements

Table 1. Summary of the Mean of Charge State Distribution (Z_{avg}) and the Charge State with Maximum Intensity (Z_{mode}) for Cytochrome *c*, Myoglobin, Lysozyme, and Ubiquitin Obtained from Both ESI and LEMS Measurements

Protein	Acid	pH	Average charge state (Z_{avg})		Average charge state with maximum intensity (Z_{mode})	
			ESI	LEMS	ESI	LEMS
Cytochrome *c*	TFA	2.2	14.5±0.1	16.3±0.3	14.2±0.4	20.0±0.6
	AA	2.9	16.2±0.1	16.5±0.5	17.9±0.4	18.8±0.9
	FA	2.5	17.8±0.1	16.8±0.3	18.2±0.5	19.8±0.4
Myoglobin	TFA	2.2	18.6±0.1	20.0±0.4	17.4±1.9	20.0±3.4
	AA	2.9	20.5±0.1	21.5±0.5	22.5±0.5	23.8±0.5
	FA	2.5	21.3±0.1	22.1±0.4	23.4±0.5	24.7±0.5
Lysozyme	TFA	2.2	11.3±0.1	11.9±0.3	11.2±0.9	12.6±0.5
	AA	2.9	11.5±0.0	11.4±0.3	11.4±0.5	11.3±0.9
	FA	2.5	12.2±0.0	11.9±0.1	13.0±0.0	11.7±0.6
Ubquitin	TFA	2.2	10.5±0.1	10.8±0.3	12.0±0.0	12.0±0.4
	AA	2.9	11.5±0.0	10.3±0.3	12.0±0.0	11.8±0.4
	FA	2.5	11.2±0.1	10.4±0.2	12.0±0.0	11.7±0.5

Table 2. Physiochemical Properties[a] of Different Electrospray Solvents

Solvent	Vapor pressure at 20°C	Boiling point (°C)	Surface tension (dyn/cm) at 20°C
Water	17.5	100	72
Methanol	97.66	64.6	22.50
Trifluoroacetic acid	97.5	73	13.63 (at 24°C)[b]
Acetic acid	11.7	117.9	27
Formic acid	44.8	101	37.67
m-NBA	1.9 (at 80°C)[c]	405[d]	50

[a] Data are taken from Ref. [62] , except as noted
[b] Data taken from Ref. [63]
[c] Data taken from Ref. [11]
[d] Data taken from Ref. [64]

were approximately the same suggests that the solution phase processes within the droplet are not important for laser vaporized protein. A droplet mixing experiment performed by colliding a 370 nL droplet of a basic solution containing phenolphthalein into an acoustically levitated 4 μL droplet of an acid showed that the basic solution remained on the surface for more than 2 s [51]. This time scale is larger than the ~100 ms time scale that the protein spends with the ES droplet during the transit to the capillary inlet in LEMS measurements. The Z_{avg} for cytochrome *c* laser vaporized into TFA and *m*-NBA is ~13% higher than for ESI. The increase in Z_{avg} is presumably due to the laser vaporization process allowing cytochrome *c* to interact exclusively with the ES droplet surface where the charge is located, eliminating interactions with the TFA anion, CF_3COO^-. The increase in Z_{avg} for LEMS measurement may also be due to the reduced protein concentration in electrospray plume. The capture efficiency of proteins is ~1% for LEMS measurements [35], which results in a higher charge availability for the given concentration of protein, resulting in a higher Z_{avg} compared with ESI. Previous CSD measurements for electrospray reveal a decrease in average charge state with increasing analyte concentration because of the decrease in excess charge with increasing protein concentration [52]. Conversely, LEMS measurements of cytochrome *c* and myoglobin did not show the same trend as a function of increasing protein concentration, suggesting minimal ion suppression compared with conventional electrospray [45]. Finally, the absolute intensities for LEMS measurements were ~80%, 74%, and 68% lower than that for ESI, for cytochrome *c* in the solution of *m*-NBA with TFA, AA, and FA, respectively. The adducts observed in the mass spectra are likely due to a reduction in desolvation of protein molecules during LEMS analysis. In the LEMS experiment, proteins are laser-vaporized from pure water, which presumably encapsulates the analyte, thereby increasing the water concentration in the droplets. In ESI, proteins are dissolved in 1:1 (v:v) water:methanol for electrospray measurements. The increase in Z_{avg} for ESI measurements using FA with *m*-NBA is probably due to the enhanced denaturation (cytochrome *c* is present in the denaturing ES for a longer time in ESI-MS) that is not present in the nonequilibrium mixing of the laser vaporized protein droplets. However, the role of *m*-NBA in the supercharging process and its effect on protein's structure has been debated [16, 18].

Myoglobin Myoglobin is a globular protein that binds heme in its hydrophobic pocket by van der Waals forces. The folded conformation with the heme group located in the interior of the protein is called holomyoglobin. The heme is released in conditions of extreme pH and/or high temperatures, and in the presence of organic solvents to produce apomyoglobin [53]. Myoglobin prepared in 1:1 (v:v) water:methanol with TFA, AA, or FA in combination with *m*-NBA was analyzed using ESI, and the mass spectra are shown in Fig. 2a, b, and c, respectively. The ESI CSD measurements are monomodal with Z_{mode} values of 19+, 22+, and 23+ for TFA, AA, and FA, respectively. The Z_{max} observed in the mass spectra was 28+ for all three electrospray solvents. The calculated Z_{mode} and Z_{avg} values for myoglobin in the solution of *m*-NBA with TFA, AA, and FA also do not correlate with the strength of the acid, as shown in Table 1. The presence of apomyoglobin features observed for all three electrospray solvents indicates a conformational change in the protein. The release of the heme cofactor is possibly due to the weakening of heme–protein interactions in the low pH (≤3.5) solution [2] and the increasing concentration of *m*-NBA during the solvent evaporation, which could further destabilize the protein structure.

Myoglobin was laser-vaporized into an electrospray solvent consisting of 1:1 (v:v) water:methanol with *m*-NBA and the various acids. The LEMS mass spectra resulting from the interaction of laser vaporized native myoglobin (holomyoglobin) with different electrospray solvents are shown in Fig. 2d, e, and f. A bimodal distribution was observed with charge states centered at 19+ and 26+ for the solution of *m*-NBA with TFA, whereas monomodal distributions centered at 23+ and 24+ were observed for the solutions of *m*-NBA with AA and FA, respectively. The Z_{max} and Z_{min} observed in the mass spectra were 28+ and 10+, respectively, for all three electrospray solvents. The ion intensity of higher charge states increases significantly for myoglobin with LEMS in comparison to ESI. The relative abundance of charge states from 19+ to 26+ for the solution of TFA and 24+ to 26+ for the solution of FA was higher for LEMS measurements compared with conventional electrospray measurements. The charge states in the mass spectra represent apomyoglobin features that resulted from the interaction of holomyoglobin with the denaturing electrospray solvent. Laser vaporization of myoglobin into the buffered water:methanol ESI displayed only holomyoglobin features (Figure S2a in Supporting

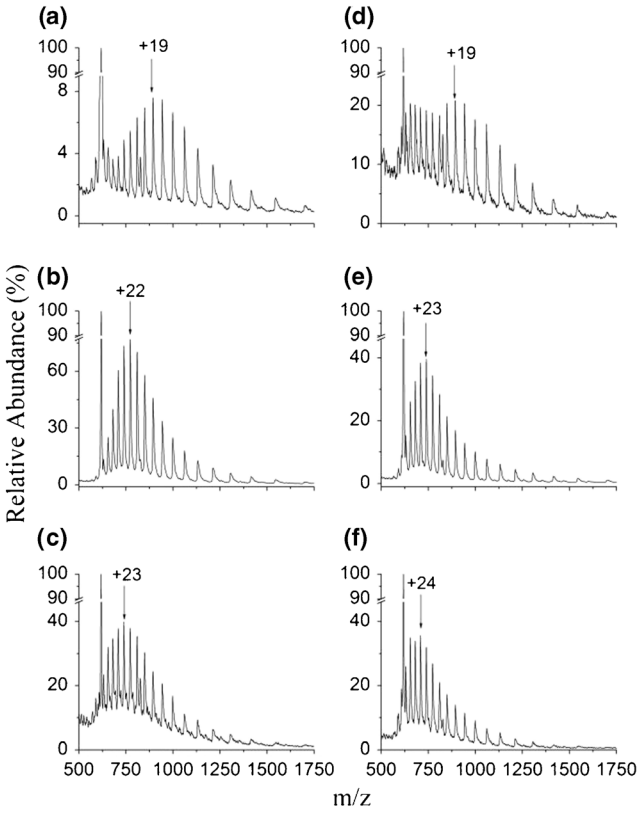

Figure 2. Mass spectra representing ES of myoglobin prepared in 1:1 (v:v) water:methanol with 0.4% *m*-NBA and 0.1% (**a**) trifluoroacetic acid, (**b**) acetic acid, and (**c**) formic acid; (**d**), (**e**), (**f**) represent laser induced vaporization of myoglobin into the ES solvent consisting of 1:1 (v:v) water:methanol with 0.4% *m*-NBA and 0.1% trifluoroacetic acid, acetic acid, and formic acid, respectively. The pH of the solution was measured to be 2.2 with trifluoroacetic acid, 2.9 with acetic acid, and 2.5 with formic acid

Information). The release of the heme cofactor indicates a conformational change of myoglobin after the laser-vaporized protein droplets interact with the denaturing ES droplets. Z_{avg} is higher for LEMS measurements than for ESI-MS, 20.0±0.4 versus 18.6±0.1 for TFA, 21.5±0.5 versus 20.5±0.1 for AA, and 22.1±0.4 versus 21.3±0.1 for FA. The increased Z_{avg} of myoglobin in LEMS measurements is similar to the observations made for cytochrome *c*, again suggesting that the laser vaporized protein acquires additional charge from the droplet surface where the excess charge resides.

Analysis of Acid-Stable Proteins (Lysozyme and Ubiquitin)

Lysozyme Lysozyme contains four disulfide bonds that stabilize the protein structure resulting in less denaturation when compared with myoglobin and cytochrome *c*. The native form of this protein is indicated by a narrow range of charge states (mostly centered at 9+ and 8+) whereas unfolded conformation displays a much broader bell-shaped distribution at higher charge states [54]. The ESI mass spectra obtained for lysozyme using the combinations of *m*-NBA and different acids are shown in Fig. 3a, b, and c. Monomodal CSDs with Z_{mode} at 11+, 12+, and 13+ were observed for *m*-NBA solutions with TFA, AA, and FA, respectively. The Z_{min} observed in the mass spectra was 8+ for all three solvent conditions, whereas the Z_{max} was 16+ for AA and FA, and 15+ for TFA solutions. The broad range of charge states ranging from 8+ to 16+ indicate an unfolded configuration of lysozyme that results from the solvents employed. The ESI mass spectra of native lysozyme prepared in buffered water:methanol solutions showed a narrow range of lower charge states with a Z_{mode} of 8+ (Figure S3c in Supporting Information). The Z_{avg} values (Table 1) measured for TFA is lower compared with AA and FA, similar to the ESI measurements of cytochrome *c* and myoglobin. Aqueous lysozyme was laser vaporized into various electrospray solutions consisting of an acidic solvent and *m*-

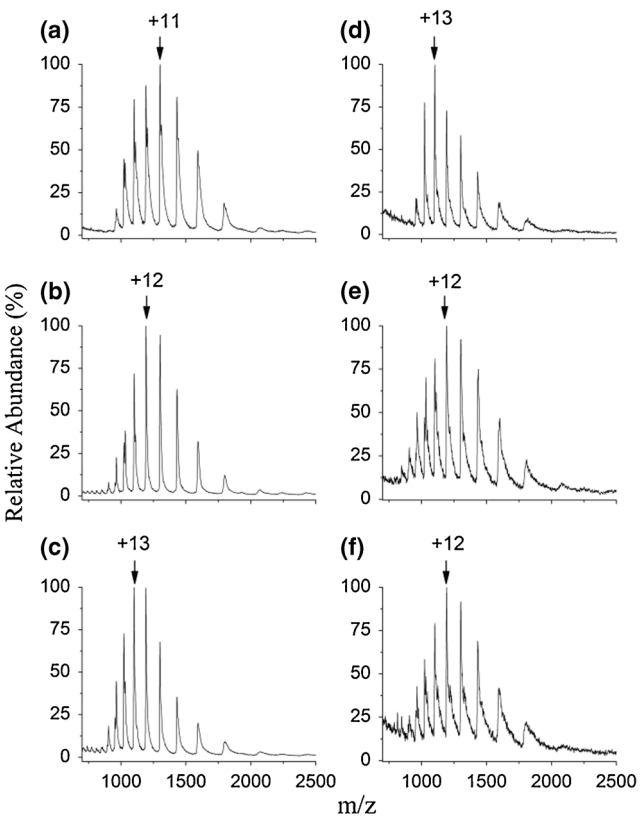

Figure 3. Mass spectra representing ES of lysozyme prepared in 1:1 (v:v) water:methanol with 0.4% *m*-NBA and 0.1% (**a**) trifluoroacetic acid, (**b**) acetic acid, and (**c**) formic acid; (**d**), (**e**), (**f**) represent laser induced vaporization of lysozyme into the ES solvent consisting of 1:1 (v:v) water:methanol with 0.4% *m*-NBA and 0.1% trifluoroacetic acid, acetic acid, and formic acid, respectively. The pH of the solution was measured to be 2.2 with trifluoroacetic acid, 2.9 with acetic acid, and 2.5 with formic acid

NBA to determine whether disulfide linkages stabilize the protein structure in the presence of denaturing electrospray solvents. The LEMS mass spectra of lyoszyme with *m*-NBA and TFA (Fig. 3d), AA (Fig. 3e), and FA (Fig. 3f) displayed monomodal CSDs. The Z_{mode} in these measurements was 13+ for the solution of TFA, and 12+ for the solutions of AA and FA (combined with *m*-NBA). The Z_{min} observed in the mass spectra was 8+ for all solvent conditions, whereas Z_{max} was 16+ for AA and FA, and 15+ for TFA solutions. The broad range of CSDs in lysozyme for all three solvent conditions indicates at least a partial change in protein structure, which occurs after the laser-vaporized protein interacts with the denaturing ES solvents containing different acids and *m*-NBA. Laser vaporization into a buffered electrospray solution containing water:methanol showed a Z_{mode} of 8+ corresponding to the folded lysozyme (Figure S3a in Supporting Information), similar to the corresponding ESI measurement. Unlike cytochrome *c* and myoglobin, the calculated Z_{avg} for LEMS measurements was slightly lower in comparison to ESI-MS measurements for FA (11.9±0.1 versus 12.2) and within the standard deviation for AA (11.4±0.3 versus 11.5), as seen in Table 1. LEMS measurements using TFA and *m*-NBA resulted in an increase Z_{avg} and Z_{mode} in comparison to ESI measurements. The slight decrease in Z_{avg} for laser-vaporized lysozyme into *m*-NBA and either FA or AA indicates a non-equilibrium interaction of the protein with the denaturing electrospray solvent. As the result of such a short interaction time with the denaturing solvent, acid-stable proteins may not denature to the same extent as the protein subjected to conventional electrospray where the protein spends a longer time in the denaturing solvent.

Lysozyme with reduced disulfide bonds was laser-vaporized into the denaturing ES containing *m*-NBA to investigate the effect of protein structure prior to mixing with the ES droplets. The LEMS mass spectra of disulfide-reduced lysozyme using the ESI solution of FA and *m*-NBA resulted in a monomodal CSD centered around 18+ (Figure S4 in Supporting Information). The Z_{max} and Z_{min} observed in the disulfide-reduced mass spectrum were 25+ and 9+, respectively. The increase in overall ion charge of the protein upon disulfide bond reduction is due to unfolding of the protein, which increases the solvent-accessible surface area, improving the protein ionization efficiency [55]. The increase in ion charge above the number of basic amino acids (18) is presumably due to the protonation of amino acids such as proline (Pro), tryptophan (Trp), and glutamine (Gln) [12, 56].

Ubiquitin Ubiquitin is a small globular protein with 76 amino-acid residues [57]. ESI measurements of the native configuration of this protein result in lower charge states (with Z_{mode} of 6+), whereas higher charge states (~11+) indicate an unfolded conformation [58]. The ESI mass spectra of ubiquitin obtained from the mixtures of *m*-NBA with the acids investigated displayed monomodal CSDs with Z_{mode} values of 12+, as observed in Fig. 4a, b, and c. The higher charge states resulting from the interaction of ubiquitin with the denaturing electrospray solutions are indicative of the unfolded conformation, whereas the lower charge states (6+ and 7+) probably represent a folded or partially folded conformation. Although there is no fluctuation in Z_{mode} (12+) for any of the solvents, the calculated Z_{avg} values vary for the different electrospray solvents and do not follow the expected trend of acid strength (10.5±0.1 (TFA), 11.5±0.03 (AA), and 11.2±0.1 (FA)). This again suggests that the nature of the protein also plays an important role in determining the Z_{avg} in addition to the acid added to the electrospray solution. The conformational flexibility and the number of ionizable groups (basic residues for positive ion mode) in a protein molecule are some of the important parameters for the observed CSD. The Z_{avg} values (Table 1) measured for myoglobin (21.3) and cytochrome *c* (17.8) were higher than lysozyme (12.2) and ubiquitin (11.2) for similar solvent conditions suggesting that the increased number of basic residues in cytochrome *c* and myoglobin favors the shift in CSD to higher charge states.

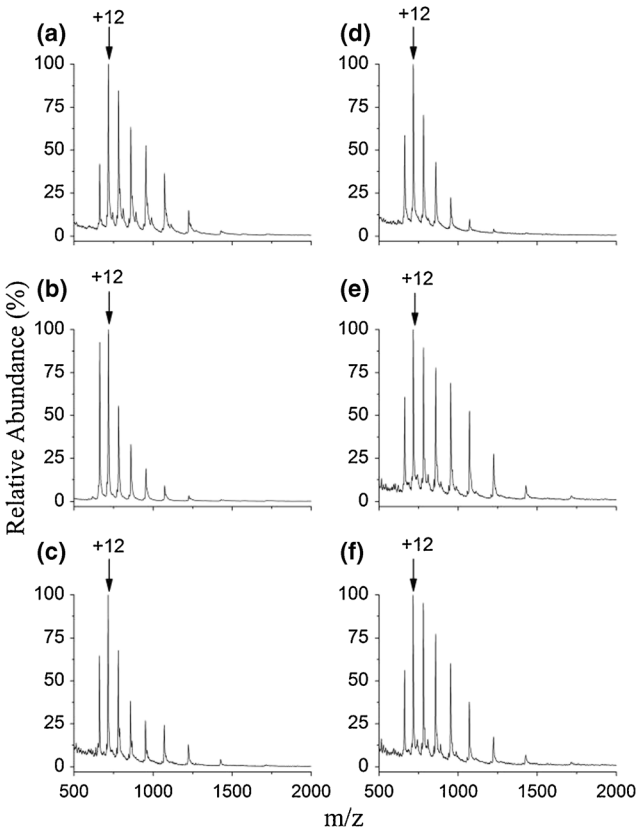

Figure 4. Mass spectra representing ES of ubiquitin prepared in 1:1 (v:v) water:methanol with 0.4% *m*-NBA and 0.1% (**a**) trifluoroacetic acid, (**b**) acetic acid, and (**c**) formic acid; (**d**), (**e**), (**f**) represent laser induced vaporization of ubiquitin into the ES solvent consisting of 1:1 (v:v) water:methanol with 0.4% *m*-NBA and 0.1% trifluoroacetic acid, acetic acid, and formic acid, respectively. The pH of the solution was measured to be 2.2 with trifluoroacetic acid, 2.9 with acetic acid, and 2.5 with formic acid

Laser vaporization of ubiquitin resulted in monomodal CSDs with Z_{mode} at 12+ for all the solvent conditions, Fig. 4 d, e, and f. The mass spectra revealed a broad range of high charge states indicating a possible denaturation of ubiquitin after the interaction of native protein with the denaturing ES solvents. The calculated Z_{avg} for LEMS was lower than ESI-MS for *m*-NBA with AA (10.3±0.3 versus 11.5±0.03) and FA (10.4±0.2 versus 11.2±0.1), but not for TFA (10.8±0.3 versus 10.5±0.1), as seen in Table 1. The decrease in Z_{avg} is possibly due to the reduced interaction time between protein and the electrospray solvent in the laser vaporization experiment in comparison with conventional electrospray, where the protein spends several minutes in the solvent. Acid-stable proteins like ubiquitin may not undergo significant denaturation during the short time (100 ms) that the protein is present in the ESI droplet after laser vaporization.

Effect of Flow Rates on Average Charge State Distribution of Cytochrome c and Myoglobin

We investigated the influence of flow rate on the charge state distributions of cytochrome *c* and myoglobin given that the charge density on the droplet surface increases for lower flow rates [59]. The protein solutions were prepared in water:methanol with *m*-NBA and either TFA or FA. The flow rate of the ES solvent was varied from 3 μL/min to 600 nL/min and the CSD was measured. The electrospray measurements of cytochrome *c* and myoglobin revealed that Z_{avg} increases as the electrospray flow rate decreases, as shown in Fig. 5. The Z_{avg} values for cytochrome *c* and myoglobin increased linearly in the solutions of *m*-NBA and TFA as the flow rate was reduced from 3 μL/min to 1 μL/min but decreased as the flow rate was further reduced to 600 nL/min. Conversely, the Z_{avg} of these proteins in the solutions of *m*-NBA and FA remained almost constant until the flow rate of 1.5 μL/min and started increasing as the flow rate decreased to 600 nL/min. The increase in Z_{avg} of the protein with decreasing flow rate is presumably due to the production of smaller electrospray droplets [60], which undergo rapid solvent evaporation, requiring fewer Coulombic fission events to generate gas phase ions [10]. This was proposed to result in an increase in surface charge density per volume of the daughter droplets compared with larger droplets generated at higher flow rates, thus improving the ionization efficiency [59]. In addition to the increase in ionization efficiency, the rate of solvent evaporation also affects the time that the protein remains in the regime of high/low surface charge density [61]. For smaller droplets, rapid solvent evaporation in the early stages of the electrospray process increases the time that protein spends in the regime of high surface charge density, contributing to the increase in high charge states in comparison with the low charge states.

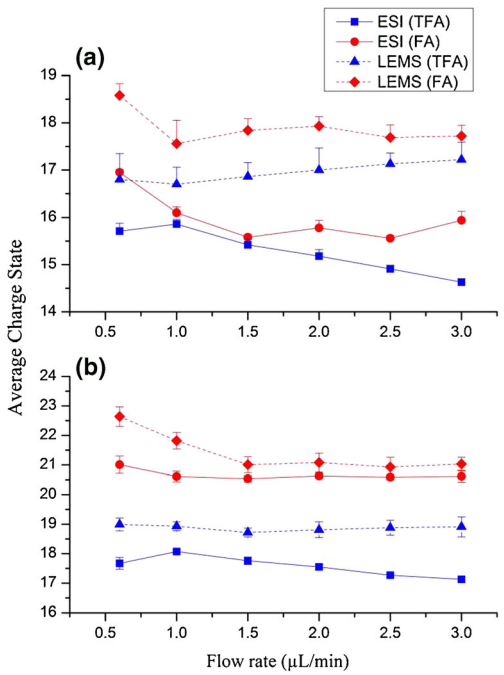

Figure 5. Plot of the average charge state of (**a**) cytochrome *c*, and (**b**) myoglobin as a function of electrospray flow rate for solvents consisting of *m*-NBA and either TFA (blue lines) or FA (red lines) for measurements using ESI-MS (solid lines) and LEMS (dashed lines)

To investigate whether the charge density on the droplet surface affected the Z_{avg} for the LEMS measurements, cytochrome *c* and myoglobin were laser-vaporized into the electrospray plume and the flow rate of the electrospray solvent was varied. The plot of Z_{avg} versus the flow rate of the electrospray solvent is shown in Fig. 5. The Z_{avg} of both proteins showed little deviation as the flow rate was reduced from 3 μL/min to 1.5 μL/min and started increasing at 1 μL/min for cytochrome *c*, and at 1.5 μL/min for myoglobin for the LEMS measurements using an ES solution of *m*-NBA with FA. However, when using the solution of *m*-NBA with TFA, the Z_{avg} remained approximately constant for myoglobin and slightly decreased for cytochrome *c* as the flow rate decreased. The decrease in Z_{avg} upon lowering the flow rate could be due to the decrease in the proton concentration on the droplet surface attributable to the lower boiling point of TFA in comparison with water. In this scenario, rapid evaporation of TFA for smaller droplets reduces the charge density on the droplet surface, thus decreasing the Z_{avg}.

Conclusions

The extent of the shift to higher charge states for proteins in the presence of denaturing solutions containing an acid and a supercharging reagent depended upon the nature of the protein, the acid, and the mass spectral technique (LEMS or ESI). The Z_{avg} values for cytochrome *c* and myoglobin were greater for LEMS measurements in comparison with ESI-MS. This is attributed to the nonequilibrium interaction of proteins with the surface of the ES droplets where the excess charge is located. The decrease in Z_{avg} with the similar solvent conditions for proteins like lysozyme and ubiquitin for LEMS measurements was attributed to their structural rigidity preventing

extensive denaturation in the acidic solution on the 100 ms timescale. The reduced interaction time of the vaporized protein with the ES plume can either enhance or limit the protein unfolding, depending on the nature of the protein and electrospray solvent. The general increase in Z_{avg} of cytochrome *c* and myoglobin with decreasing flow rate (3 μL/min to 600 nL/min) was attributed to the production of smaller droplets compared with higher flow rates experiments. The more rapid solvent evaporation for smaller droplets in the early stages of the electrospray process increases the time protein spends in the regime of high surface charge density, contributing to the increase in ion abundance of high charge states.

The combination of *m*-NBA and formic acid resulted in the highest average charge states for proteins in both ESI-MS and LEMS measurements. This is presumably due to the increase in proton density on the droplet surface, which improves the ionization efficiency of the proteins. Further, increase in both the Z_{avg} and the Z_{mode} values for LEMS measurements compared with conventional electrospray for acid-sensitive proteins like cytochrome *c* and myoglobin suggest that LEMS could be utilized to create higher charge states for performing top-down tandem mass spectrometry on proteins. The ability to vaporize and ionize multiple components irrespective of chemical functionality from complex mixtures without the addition of matrix illustrates the potential of LEMS for various applications, such as imaging mass spectrometry, quantitative measurements of biological samples, forensic analysis, etc. With the advances in laser technology, the measurements can now be performed using a commercial fiber laser, which is turnkey and affordable.

Acknowledgements

The work was supported by the National Science Foundation (CHE 0957694).

References

1. Konermann, L., Douglas, D.: Acid-induced unfolding of cytochrome c at different methanol concentrations: electrospray ionization mass spectrometry specifically monitors changes in the tertiary structure. Biochemistry **36**, 12296–12302 (1997)
2. Chowdhury, S.K., Katta, V., Chait, B.T.: Probing conformational changes in proteins by mass spectrometry. J. Am. Chem. Soc. **112**, 9012–9013 (1990)
3. Iavarone, A.T., Jurchen, J.C., Williams, E.R.: Effects of solvent on the maximum charge state and charge state distribution of protein ions produced by electrospray ionization. J. Am. Soc. Mass Spectrom. **11**, 976–985 (2000)
4. Loo, R.R.O., Smith, R.D.: Proton transfer reactions of multiply charged peptide and protein cations and anions. J. Mass Spectrom. **30**, 339–347 (1995)
5. Williams, E.R.: Proton transfer reactivity of large multiply charged ions. J. Mass Spectrom. **31**, 831 (1996)
6. Flick, T.G., Williams, E.R.: Supercharging with trivalent metal ions in native mass spectrometry. J. Am. Soc. Mass Spectrom. **23**, 1885–1895 (2012)
7. Iavarone, A.T., Jurchen, J.C., Williams, E.R.: Supercharged protein and peptide ions formed by electrospray ionization. Anal. Chem. **73**, 1455–1460 (2001)
8. Lomeli, S.H., Peng, I.X., Yin, S., Ogorzalek Loo, R.R., Loo, J.A.: New reagents for increasing ESI multiple charging of proteins and protein complexes. J. Am. Soc. Mass Spectrom. **21**, 127–131 (2010)
9. Sterling, H.J., Prell, J.S., Cassou, C.A., Williams, E.R.: Protein conformation and supercharging with DMSO from aqueous solution. J. Am. Soc. Mass Spectrom. **22**, 1178–1186 (2011)
10. Page, J.S., Kelly, R.T., Tang, K., Smith, R.D.: Ionization and transmission efficiency in an electrospray ionization-mass spectrometry interface. J. Am. Soc. Mass Spectrom. **18**, 1582–1590 (2007)
11. Banerjee, S.: Induction of protein conformational change inside the charged electrospray droplet. J. Mass Spectrom. **48**, 193–204 (2013)
12. Kharlamova, A., Prentice, B.M., Huang, T.-Y., McLuckey, S.A.: Electrospray droplet exposure to gaseous acids for the manipulation of protein charge state distributions. Anal. Chem. **82**, 7422–7429 (2010)
13. Chen, H., Touboul, D., Jecklin, M.C., Zheng, J., Luo, M., Zenobi, R.: Manipulation of charge states of biopolymer ions by atmospheric pressure ion/molecule reactions implemented in an extractive electrospray ionization source. Eur. J. Mass Spectrom. **13**, 273 (2007)
14. Touboul, D., Jecklin, M.C., Zenobi, R.: Investigation of deprotonation reactions on globular and denatured proteins at atmospheric pressure by ESSI-MS. J. Am. Soc. Mass Spectrom. **19**, 455–466 (2008)
15. Hogan Jr., C.J., Ogorzalek Loo, R.R., Loo, J.A., de la Mora, J.F.: Ion mobility-mass spectrometry of phosphorylase B ions generated with supercharging reagents but in charge-reducing buffer. Phys. Chem. Chem. Phys. **12**, 13476–13483 (2010)
16. Lomeli, S.H., Yin, S., Ogorzalek Loo, R.R., Loo, J.A.: Increasing charge while preserving noncovalent protein complexes for ESI-MS. J. Am. Soc. Mass Spectrom. **20**, 593–596 (2009)
17. Sterling, H.J., Cassou, C.A., Trnka, M.J., Burlingame, A., Krantz, B.A., Williams, E.R.: The role of conformational flexibility on protein supercharging in native electrospray ionization. Phys. Chem. Chem. Phys. **13**, 18288–18296 (2011)
18. Sterling, H.J., Williams, E.R.: Origin of supercharging in electrospray ionization of noncovalent complexes from aqueous solution. J. Am. Soc. Mass Spectrom. **20**, 1933–1943 (2009)
19. Hall, Z., Robinson, C.V.: Do charge state signatures guarantee protein conformations? J. Am. Soc. Mass Spectrom. **23**, 1161–1168 (2012)
20. Marshall, A.G.: Fourier transform ion cyclotron resonance mass spectrometry. Acc. Chem. Res. **18**, 316–322 (1985)
21. Perry, R.H., Cooks, R.G., Noll, R.J.: Orbitrap mass spectrometry: instrumentation, ion motion and applications. Mass Spectrom. Rev. **27**, 661–699 (2008)
22. Good, D.M., Wirtala, M., McAlister, G.C., Coon, J.J.: Performance characteristics of electron transfer dissociation mass spectrometry. Mol. Cell Proteomics **6**, 1942–1951 (2007)
23. Horn, D.M., Breuker, K., Frank, A.J., McLafferty, F.W.: Kinetic intermediates in the folding of gaseous protein ions characterized by electron capture dissociation mass spectrometry. J. Am. Chem. Soc. **123**, 9792–9799 (2001)
24. Tsybin, Y.O., Fornelli, L., Stoermer, C., Luebeck, M., Parra, J., Nallet, S., Wurm, F.M., Hartmer, R.: Structural analysis of intact monoclonal antibodies by electron transfer dissociation mass spectrometry. Anal. Chem. **83**, 8919–8927 (2011)
25. Zubarev, R.A., Kelleher, N.L., McLafferty, F.W.: Electron capture dissociation of multiply charged protein cations. A nonergodic process. J. Am. Chem. Soc. **120**, 3265–3266 (1998)
26. Zubarev, R.A., Horn, D.M., Fridriksson, E.K., Kelleher, N.L., Kruger, N.A., Lewis, M.A., Carpenter, B.K., McLafferty, F.W.: Electron capture dissociation for structural characterization of multiply charged protein cations. Anal. Chem. **72**, 563–573 (2000)
27. Peng, I.X., Ogorzalek Loo, R.R., Shiea, J., Loo, J.A.: Reactive-electrospray-assisted laser desorption/ionization for characterization of peptides and proteins. Anal. Chem. **80**, 6995–7003 (2008)
28. Nemes, P., Vertes, A.: Laser ablation electrospray ionization for atmospheric pressure, in vivo, and imaging mass spectrometry. Anal. Chem. **79**, 8098–8106 (2007)
29. Rezenom, Y.H., Dong, J., Murray, K.K.: Infrared laser-assisted desorption electrospray ionization mass spectrometry. Analyst **133**, 226–232 (2008)
30. Sampson, J.S., Muddiman, D.C.: Atmospheric pressure infrared (10.6 μm) laser desorption electrospray ionization (IR-LDESI) coupled to a LTQ Fourier transform ion cyclotron resonance mass spectrometer. Rapid Commun. Mass Spectrom. **23**, 1989–1992 (2009)
31. Liu, J., Qiu, B., Luo, H.: Fingerprinting of yogurt products by laser desorption spray post-ionization mass spectrometry. Rapid Commun. Mass Spectrom. **24**, 1365–1370 (2010)

32. Sampson, J.S., Hawkridge, A.M., Muddiman, D.C.: Construction of a versatile high precision ambient ionization source for direct analysis and imaging. J. Am. Soc. Mass Spectrom. **19**, 1527–1534 (2008)
33. Flanigan, P., Levis, R.: Ambient femtosecond laser vaporization and nanosecond laser desorption electrospray ionization mass spectrometry. Annu. Rev. Anal. Chem. **7**, 229–256 (2014)
34. Brady, J.J., Judge, E.J., Levis, R.J.: Mass spectrometry of intact neutral macromolecules using intense non-resonant femtosecond laser vaporization with electrospray post-ionization. Rapid Commun. Mass Spectrom. **23**, 3151–3157 (2009)
35. Judge, E.J., Brady, J.J., Dalton, D., Levis, R.J.: Analysis of pharmaceutical compounds from glass, fabric, steel, and wood surfaces at atmospheric pressure using spatially resolved, nonresonant femtosecond laser vaporization electrospray mass spectrometry. Anal. Chem. **82**, 3231–3238 (2010)
36. Brady, J.J., Judge, E.J., Levis, R.J.: Analysis of amphiphilic lipids and hydrophobic proteins using nonresonant femtosecond laser vaporization with electrospray post-ionization. J. Am. Soc. Mass Spectrom. **22**, 762–772 (2011)
37. Brady, J.J., Judge, E.J., Simon, K., Levis, R.J.: Presented in part at the Proceedings of SPIE 7568. Imaging Manip. Anal. Biomol. Cells Tissues VIII (2010)
38. Brady, J.J., Judge, E.J., Levis, R.J.: Identification of explosives and explosive formulations using laser electrospray mass spectrometry. Rapid Commun. Mass Spectrom. **24**, 1659–1664 (2010)
39. Flanigan IV, P.M., Brady, J.J., Judge, E.J., Levis, R.J.: Determination of inorganic improvised explosive device signatures using laser electrospray mass spectrometry detection with offline classification. Anal. Chem. **83**, 7115–7122 (2011)
40. Perez, J.J., Flanigan IV, P.M., Brady, J.J., Levis, R.J.: Classification of smokeless powders using laser electrospray mass spectrometry and offline multivariate statistical analysis. Anal. Chem. **85**, 296–302 (2012)
41. Flanigan IV, P.M., Radell, L.L., Brady, J.J., Levis, R.J.: Differentiation of eight phenotypes and discovery of potential biomarkers for a single plant organ class using laser electrospray mass spectrometry and multivariate statistical analysis. Anal. Chem. **84**, 6225–6232 (2012)
42. Judge, E.J., Brady, J.J., Barbano, P.E., Levis, R.J.: Nonresonant femtosecond laser vaporization with electrospray postionization for ex vivo plant tissue typing using compressive linear classification. Anal. Chem. **83**, 2145–2151 (2011)
43. Brady, J.J., Judge, E.J., Levis, R.J.: Nonresonant femtosecond laser vaporization of aqueous protein preserves folded structure. Proc. Natl. Acad. Sci. **108**, 12217–12222 (2011)
44. Flanigan IV, P.M., Perez, J.J., Karki, S., Levis, R.J.: Quantitative measurements of small molecule mixtures using laser electrospray mass spectrometry. Anal. Chem. **85**, 3629–3637 (2013)
45. Perez, J.J., Flanigan, P.M., Karki, S., Levis, R.J.: Laser electrospray mass spectrometry minimizes ion suppression facilitating quantitative mass spectral response for multi-component mixtures of proteins. Anal. Chem. **85,** 6667–6673 (2013)
46. Shackman, J.G., Watson, C.J., Kennedy, R.T.: High-throughput automated post-processing of separation data. J. Chromatogr. A **1040**, 273–282 (2004)
47. Fligge, T.A., Kast, J., Bruns, K., Przybylski, M.: Direct monitoring of protein–chemical reactions utilizing nanoelectrospray mass spectrometry. J. Am. Soc. Mass Spectrom. **10**, 112–118 (1999)
48. Valentine, S.J., Clemmer, D.E.: H/D exchange levels of shape-resolved cytochrome *c* conformers in the gas phase. J. Am. Chem. Soc. **119**, 3558–3566 (1997)
49. Mirza, U.A., Chait, B.T.: Effects of anions on the positive ion electrospray ionization mass spectra of peptides and proteins. Anal. Chem. **66**, 2898–2904 (1994)
50. Liu, X., Cole, R.B.: A new model for multiply charged adduct formation between peptides and anions in electrospray mass spectrometry. J. Am. Soc. Mass Spectrom. **22**, 2125–2136 (2011)
51. Chainani, E.T., Choi, W.-H., Ngo, K.T., Scheeline, A.: Mixing in colliding ultrasonically levitated drops. Anal. Chem. **86,** 2229–2237 (2014)
52. Wang, G., Cole, R.B.: Mechanistic interpretation of the dependence of charge state distributions on analyte concentrations in electrospray ionization mass spectrometry. Anal. Chem. **67**, 2892–2900 (1995)
53. Creighton, T.E.: Proteins: structures and molecular properties. W.H. Freeman & Co, New York (1993)
54. Gross, D.S., Schnier, P.D., Rodriguez-Cruz, S.E., Fagerquist, C.K., Williams, E.R.: Conformations and folding of lysozyme ions in vacuo. Proc. Natl. Acad. Sci. **93**, 143–3148 (1996)
55. Testa, L., Brocca, S., Grandori, R.: Charge-surface correlation in electrospray ionization of folded and unfolded proteins. Anal. Chem. **83**, 6459–6463 (2011)
56. Schnier, P.D., Gross, D.S., Williams, E.R.: On the maximum charge state and proton transfer reactivity of peptide and protein ions formed by electrospray ionization. J. Am. Soc. Mass Spectrom. **6**, 1086–1097 (1995)
57. Vijay-Kumar, S., Bugg, C.E., Cook, W.J.: Structure of ubiquitin refined at 1.8 Å resolution. J. Mol. Biol. **194**, 531–544 (1987)
58. Konermann, L., Douglas, D.: Unfolding of proteins monitored by electrospray ionization mass spectrometry: a comparison of positive and negative ion modes. J. Am. Soc. Mass Spectrom. **9**, 1248–1254 (1998)
59. Schmidt, A., Karas, M., Dülcks, T.: Effect of different solution flow rates on analyte ion signals in nano-ESI MS, or: when does ESI turn into nano-ESI? J. Am. Soc. Mass Spectrom. **14**, 492–500 (2003)
60. Ganan-Calvo, A., Davila, J., Barrero, A.: Current and droplet size in the electrospraying of liquids. Scaling laws. J. Aerosol Sci. **28**, 249–275 (1997)
61. Fenn, J.B.: Ion formation from charged droplets: roles of geometry, energy, and time. J. Am. Soc. Mass Spectrom. **4**, 524–535 (1993)
62. Frederikse, H., Lide, D.: CRC handbook of chemistry and physics. Boca Raton, CRC (1996)
63. Jasper, J.J., Wedlick, H.L.: Effect of Temperature on the surface tension and density of trifluoroacetic acid. J. Chem. Eng. Data **9**, 446–447 (1964)
64. Goodman, J.M., Kirby, P.D., Haustedt, L.O.: Some calculations for organic chemists: boiling point variation, Boltzmann factors, and the Eyring equation. Tetrahedron Lett. **41**, 9879–9882 (2000)